

The short-time limit of the Dirichlet partition function and the image method

Agapitos Hatzinikitas

University of Aegean,
School of Sciences,
Department of Mathematics,
Karlovasi, 83200
Samos Greece
Email: ahatz@aegean.gr

Abstract

In this paper we calculate the short-time limit of the free partition function for a diffusion process on tessellations of the n -dimensional Euclidean space \mathbb{E}^n , $n = 1, 2, 3$ with an absorbing boundary. Utilising the method of images for domains which are compatible with finite reflection subgroups of the orthogonal group \mathbb{O}_n we recover old results from a different viewpoint and produce new ones.

1 Introduction

In 1954 Pleijel [16] established the formula

$$\sum_{m=1}^{\infty} e^{-\lambda_m t} \underset{t \rightarrow 0^+}{\sim} \frac{|\Omega|}{4\pi t} - \frac{|\partial\Omega|}{8\sqrt{\pi t}} + \frac{1}{6} \quad (1)$$

for simply connected domains with surface area $|\Omega|$ and length of the perimeter $|\partial\Omega|$ in \mathbb{R}^2 . Later Kac [9] using a combination of probability techniques with heat equation methods justified the first two terms in (1) for convex domains and obtained the third term as a limiting case of convex polygonal domains. He also conjectured for multiply connected subdomains in \mathbb{R}^2 with h -holes that the time independent term should be replaced by $(1-h)/6$. McKean and Singer [13] generalised (1) for smooth compact n -dimensional Riemannian manifolds (Ω, g) with or without $(n-1)$ -dimensional Lebesgue measure of its boundary $\partial\Omega$. They proved for Dirichlet boundary conditions that the coefficients c_0, c_1, c_2 in the expansion

$$Z_{\Omega}(t) = \frac{1}{(4\pi t)^{\frac{n}{2}}} \sum_{m=0}^l c_m t^{\frac{m}{2}} + o(t^{\frac{l+1}{2}}) \quad (2)$$

are given by

$$c_0 = |\Omega|, \quad c_1 = -\frac{\pi}{2}|\partial\Omega|, \quad c_3 = \frac{1}{3} \int_{\Omega} K - \frac{1}{6} \int_{\partial\Omega} J \quad (3)$$

where K is the scalar curvature (the negative spur of the Ricci tensor) and J the mean curvature (the trace of the second fundamental form) at a point on $\partial\Omega$.

In the present paper we study the short-time asymptotics of (2) applying the image method in $n = 1, 2, 3$ dimensions. The power of this method is based on the connection between the heat kernel in Ω and the heat kernel in \mathbb{E}^n through the reflection group. The explicit knowledge of the spectrum of the Dirichlet Laplacian which conveys all the geometrical information of the domain is redundant. Although the main obstruction to the eigenvalue problem of the Dirichlet Laplacian seems to be the failure of separation of variables, techniques have been developed to overcome this difficulty at least to some particular cases [7, 8, 12].

In Section 2 we recall some well known results related to the partition function in the $t \rightarrow 0^+$ limit and prove an incidental formula (15) which exhibits the geometrical origin of the topological term for polygonal

boundaries in $n = 2$. We also explain the way one can construct the Green's function for an open and bounded domain from the corresponding Green's function of the unbounded space.

In Section 3 we compute $Z_\Omega(t)$ in the $t \rightarrow 0^+$ limit for $n = 1$ and study the more interesting two- and three-dimensional cases. The problem of classifying all the bounded domains allowed by the image method was partly solved in [11]. To determine the short-time asymptotics of the transition probability we stood on Coxeter's work [1, 2] on discrete groups (see also [10] for an updated treatment of the subject) which are related to the classification of semi-simple Lie algebras according to Cartan and Weyl. Working in this direction for the infinite two-dimensional wedge we observe that only elements of the cyclic subgroup of the dihedral group contribute to the topological term. In the short-time limit the result is insensitive under truncation of the wedge. Therefore Kac's result for simply connected domains in $n = 2$ is justified. Repeating the same procedure for the infinite trihedral $(2, 2, r)$ case in three dimensions we find a closed formula for the corresponding topological term. We classify tessellations which are compatible with the image method and specify their $Z_\Omega(t)$. It is worth noting that the asymptotic partition function of the hyperrectangle in n -dimensions is possibly the only concrete result we have at present.

2 Theoretical Background

In this section we explain the theoretical background needed to understand the concept of short-time asymptotics of the partition function as well as the reason for which the method of images is applicable in determining the trace of the Dirichlet heat kernel.

Let us consider the diffusion equation ¹

$$\frac{\partial P_t(x, y)}{\partial t} = \mathcal{D} \Delta_{D, x} P_t(x, y) \quad \text{in } \mathbb{R}_+ \times \Omega, \quad P_t(x, y) \equiv P_\Omega(x, y; t) \quad (4)$$

where $\mathcal{D} > 0$ is the diffusion constant with dimensions $[L^2 T^{-1}]$, Ω an open, bounded and simply connected subset of \mathbb{R}^n with boundary $\partial\Omega$ and Δ_D the Dirichlet Laplace operator. The parabolic partial differential equation (4) is subjected to the initial condition

$$\lim_{t \rightarrow 0^+} \int_{\Omega} P_t(x, y) dx = 1 \quad (5)$$

and to the homogeneous Dirichlet boundary condition

$$\lim_{x \rightarrow q \in \partial\Omega} P_t(x, y) = 0, \quad \forall y \in \Omega. \quad (6)$$

The physical context of (5) is the existence of a point source initially described by a generalized Dirac- δ function while (6) dictates that the process is killed upon reaching the boundary. In the unbounded case the solution of (4) equipped with (5) is the Gauss-Weierstrass function (or heat kernel or transition density or propagator) given, for $\mathcal{D} = 1$, by

$$P_{0,t}(x, y) = P_{0,t}(d(x, y)) = \frac{1}{(4\pi t)^{n/2}} e^{-\frac{d^2(x, y)}{4t}}, \quad t > 0, \quad x, y \in \mathbb{R}^n \quad (7)$$

where $d(x, y) = \|x - y\| = \sqrt{\sum_{i=1}^n (x_i - y_i)^2}$ is the Euclidean distance between two points on \mathbb{R}^n . It can be proved [3] that the semigroup $\{e^{t\Delta_D}\}_{t \geq 0}$ on $L^2(\Omega)$ has a strictly positive C^∞ kernel on $(0, \infty) \times \Omega \times \Omega$ which satisfies

$$0 < P_t(x, y) \leq P_{0,t}(x, y) \quad \forall t > 0, \quad x, y \in \Omega. \quad (8)$$

¹In this equation x represents the location of the observation point while y stands for the location of the point source.

Let us denote by $|\Omega|$ the n -dimensional Lebesgue measure of Ω , then from (8), it follows that the mapping $e^{t\Delta_D} : L^2(\Omega) \rightarrow L^\infty(\Omega)$ is of trace class with

$$0 < Z_\Omega(t) = \text{Tr}_\Omega(e^{t\Delta_D}) = \int_\Omega P_t(x, x) dx \leq \frac{P_{0,t=1}(0)}{t^{n/2}} |\Omega| \quad (9)$$

where $P_{0,t=1}(0) = \frac{\omega_n \Gamma(n/2)}{2(2\pi)^n}$ with $\omega_n = \frac{2\pi^{n/2}}{\Gamma(n/2)}$ the surface of the unit sphere \mathbb{S}^{n-1} . The quantity Z_Ω is usually referred as the partition function of Ω . In fact there exists a total orthonormal set of eigenfunctions $\{\psi_m\}_{m=1}^\infty \in L^2(\Omega)$ and corresponding eigenvalues $\{\lambda_m\}_{m=1}^\infty$ of the generator of the semigroup such that

$$\begin{aligned} e^{t\Delta_D} \psi_m(x) &= e^{-\lambda_m t} \psi_m(x), \quad x \in \Omega, t > 0 \\ 0 < \lambda_1 &\leq \lambda_2 \leq \lambda_3 \leq \dots \end{aligned} \quad (10)$$

with infinity as accumulation point. Under such assumptions we have

$$P_t(x, y) = \sum_{m=1}^\infty e^{-\lambda_m t} \psi_m(x) \bar{\psi}_m(y). \quad (11)$$

Because of (11), we can rewrite the partition function in terms of the eigenvalues λ_m as follows

$$Z_\Omega(t) = \sum_{m=1}^\infty e^{-\lambda_m t} \int_\Omega \psi_m(x) \bar{\psi}_m(x) dx = \sum_{m=1}^\infty e^{-\lambda_m t}. \quad (12)$$

We are interested in the asymptotic behaviour of the trace of the semigroup $\{e^{t\Delta_D}\}_{t \geq 0}$ as $t \rightarrow 0^+$ when Ω is a tessellation² which is generated by reflections through the hyperplanes bounding the fundamental region.

In one dimension the behaviour of the trace of the heat kernel is given by

$$Z_\Omega(t) \stackrel{t \rightarrow 0^+}{\sim} \frac{|\Omega|}{2\sqrt{\pi t}} - \frac{1}{2} \quad (13)$$

while for a polytope³ in two dimensions with N vertices is

$$Z_\Omega(t) \stackrel{t \rightarrow 0^+}{\sim} \frac{|\Omega|}{4\pi t} - \frac{|\partial\Omega|}{8\sqrt{\pi t}} + \sum_{i=1}^N \frac{\pi^2 - \phi_i^2}{24\pi\phi_i} \quad (14)$$

for arbitrary angles $0 < \phi_i < 2\pi$, $i = 1, \dots, N$. The last term in (14), which is of topological origin, can be written alternatively in terms of the curvature k_{ν_i} at the vertex ν_i (see Appendix A for the proof) of the polygon as

$$\sum_{i=1}^N \frac{\pi^2 - \phi_i^2}{24\pi\phi_i} = -\frac{(N-2)}{24} + \frac{\pi}{24} \sum_{i=1}^N \frac{1}{\pi - k_{\nu_i}}. \quad (15)$$

In n -dimensions the general expression for a hyperrectangle is [6]

$$\begin{aligned} Z_\Omega(t) &\stackrel{\text{as } t \rightarrow 0^+}{\sim} \sum_{m=0}^n \left(\frac{1}{\pi t^{\frac{1}{2}}} \Gamma\left(1 + \frac{1}{2}\right) \right)^m \left(-\frac{1}{2} \right)^{n-m} V_m(\Omega) \\ &= \left(\frac{1}{\pi t^{\frac{1}{2}}} \Gamma\left(1 + \frac{1}{2}\right) \right)^n V_n(\Omega) + \sum_{r=0}^{n-1} \left(\frac{1}{\pi t^{\frac{1}{2}}} \Gamma\left(1 + \frac{1}{2}\right) \right)^{n-r} \left(-\frac{1}{2} \right)^r \frac{n-r}{O_{n-r-1}} \binom{n}{n-r} W_{n-r}(\Omega) \end{aligned} \quad (16)$$

²A tessellation is an infinite set of polygons (or polyhedra) fitting together to cover the plane (or space) just once, so that every side (or face) of each polygon (or polyhedron) belongs also to one other polygon (or polyhedron).

³A polyhedral set is the intersection of a finite number of closed half-spaces. Bounded polyhedra are called polytopes.

where V_m, W_{n-r} are the m th intrinsic volume and quermassintegral. The topological term in arbitrary dimension and for a general polytope cannot be determined in closed form. It is worth noting that

$$\lim_{t \rightarrow 0^+} t^{n/2} Z_\Omega(t) = C_1 |\Omega| \quad (17)$$

where $C_1 = P_{0,t=1}(0)$ and (17) holds without assuming that $\partial\Omega$ has finite volume.

Remark

The heat kernel in \mathbb{R}^n is invariant under the action of the group of isometries of the affine Euclidean space which is a semidirect product of the group \mathbb{R}^n of all translations and the orthogonal group \mathbb{O}_n . Moreover under the dilatations $\Omega' = \rho\Omega$, $\rho \in \mathbb{R}^+$ and $t' = \rho^2 t$ the heat kernel in Ω transforms according to

$$P_{t'}(x', y') = \rho^{-n} P_t(x, y) \quad (18)$$

since the eigenvalues and eigenstates of the Dirichlet Laplacian scale like $\lambda'_m = \rho^{-2} \lambda_m$ and $\psi'_m(x') = \rho^{-n/2} \psi_m(x)$ respectively. Therefore the partition function is scale invariant by (12) and using the isometries of the Euclidean space one can recover its short-time asymptotic behaviour given by (2).

Our objective is to reproduce (13), (14) and extend this result in \mathbb{R}^3 wherever it is tractable. For this let us study, using the method of images, the Dirichlet Green's function defined by

$$-\Delta_x G_\Omega(x, y) = \delta(x - y), \quad x, y \in \Omega \quad (19)$$

$$G_\Omega(x, y) = 0, \quad x \in \partial\Omega. \quad (20)$$

The solution of the previous boundary problem can be expressed as an alternating sum of Green's functions in the unbounded space with virtual point sources generated by reflecting anticlockwise (or clockwise) the initial point source at y through the hyperplanes bounding Ω . Note that since Ω is a tessellation of the space there is a one-to-one correspondence between the virtual source points and the images of Ω under the action of the reflection group. Thus we obtain

$$G_\Omega(x, y) = \sum_{s=0}^{\infty} (-1)^s G_0(x, R_{a_s} y), \quad x \in \Omega, y \in R_{a_s} \Omega \quad (21)$$

where s, R_{a_s} denote the order (number of reflections) and the element associated with the corresponding reflection. As an example consider the triangular domain which has $3 \times 2^{p-1}$ reflections of order p . One can check that (21) satisfies both (19) and (20). The connection of the Green's function with the heat kernel is given by

$$G_\Omega(x, y) = \int_0^\infty P_t(\|x - y\|) dt, \quad x, y \in \Omega \quad (22)$$

which when combined with (11) reproduces the well-known expansion

$$G_\Omega(x, y) = \sum_{m=1}^{\infty} \frac{1}{\lambda_m} \psi_m(x) \bar{\psi}_m(y). \quad (23)$$

The asymptotic behaviour of the Dirichlet partition function in the $t \rightarrow 0^+$ limit is dominated by the diagonal elements of the heat kernel which receive contributions from the heat kernels of the unbounded space for the virtual source points clustering around each vertex of the polytope (see figure (4)). The corresponding expression is

$$\lim_{x \rightarrow y} P_t^v(x, y) \stackrel{t \rightarrow 0^+}{\sim} \sum_{s=0}^{|\mathcal{G}_v|} (-1)^s P_{0,t}(\|(I - R_{a_{s_v}})y\|) \quad (24)$$

where $|\mathcal{G}_v|$ is the order of the reflection group at vertex v . Thus integrating (24) over a suitable subdomain of Ω and then taking the $t \rightarrow 0^+$ limit we recover (13) and (14).

3 The $Z_\Omega(t)$ in the $t \rightarrow 0^+$ limit

3.1 The $n = 1$ case

In $n = 1$, \mathcal{G} coincides to the infinite dihedral group Dih_∞ with defining relations

$$R_{a_1}^2 = R_{a_2}^2 = I \quad (25)$$

where R_{a_i} 's are involuntary transformations and represent reflections w.r.t. the boundary points of $\Omega \subset \mathbb{R}$. Assuming that $\Omega = (0, L)$ for every $y \in \Omega$ we generate the following two infinite sequences of virtual source points depending on whether we start reflection from the left or right fixed point of the isometry R_i .

The virtual image points of y			
Left fixed point		Right fixed point	
Group Element	Location of virtual image point	Group Element	Location of virtual image point
R_{a_2}	$-y$	R_{a_1}	$-y+2L$
$R_{a_1} \cdot R_{a_2}$	$y+2L$	$R_{a_2} \cdot R_{a_1}$	$y-2L$
$R_{a_2} \cdot R_{a_1} \cdot R_{a_2}$	$-y-2L$	$R_{a_1} \cdot R_{a_2} \cdot R_{a_1}$	$-y+4L$
$(R_{a_1} \cdot R_{a_2})^2$	$y+4L$	$(R_{a_2} \cdot R_{a_1})^2$	$y-4L$
\vdots	\vdots	\vdots	\vdots

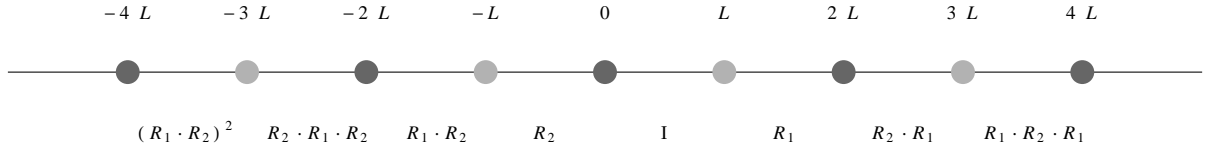
(26)


Figure 1: The fundamental region $\Omega = (0, L)$ and the virtual domains generated by the elements $R_i \equiv R_{a_i}$ of the infinite dihedral group.

The heat kernel in this case is written as

$$P_t(x, y) = P_0(\|x - y\|) - \sum_{n \in \mathbb{Z}} P_0(\|x + y + 2nL\|) + \sum_{n \in \mathbb{Z} \setminus \{0\}} P_0(\|x - y + 2nL\|) \quad (27)$$

where, after reordering, we gather in the first sum the contribution of odd number of group elements while in the second sum that of even number of group elements. Relation (24) becomes

$$P_t(y, y) = \frac{1}{\sqrt{4\pi t}} \left(1 - \sum_{n \in \mathbb{Z}} e^{-\frac{\|y+nL\|^2}{t}} + 2 \sum_{n \in \mathbb{N} \setminus \{0\}} e^{-\frac{\|nL\|^2}{t}} \right) \quad (28)$$

which after integration over the fundamental domain, taking the $t \rightarrow 0^+$ limit and maintaining $t^{-1/2}$ terms we obtain

$$\begin{aligned} Z_\Omega(t) &\sim \frac{1}{\sqrt{4\pi t}} \int_0^L dy - \lim_{t \rightarrow 0^+} \left(\frac{1}{\sqrt{4\pi t}} \sum_{n \in \mathbb{Z}} \int_0^L e^{-\frac{\|y+nL\|^2}{t}} dy \right) + 2 \lim_{t \rightarrow 0^+} \left(\frac{1}{\sqrt{4\pi t}} \sum_{n \in \mathbb{N} \setminus \{0\}} \int_0^L e^{-\frac{\|nL\|^2}{t}} dy \right) \\ &= \frac{L}{\sqrt{4\pi t}} - 2 \lim_{t \rightarrow 0^+} \left(\frac{1}{4} \text{erf} \left(\frac{L}{\sqrt{t}} \right) \right) + \sum_{n \in \mathbb{N} \setminus \{0\}} \delta(n) \\ &= \frac{L}{\sqrt{4\pi t}} - \frac{1}{2}. \end{aligned} \quad (29)$$

3.2 The $n = 2$ case

The case $n = 2$ is more involved. Let θ be the angle between two intersecting mirrors in \mathbb{R}^2 . If we require the absence of a virtual mirror between the two given ones, after successive reflections of the fundamental domain, then $\theta = \frac{\pi}{q}$ where $q \in \mathbb{N} \setminus \{1, 2\}$. This remark facilitates the enumeration of bounded tessellations of the plane through reflections. For triangular domains with angles $\pi/p, \pi/q, \pi/r$; $p, q, r \in \mathbb{N} \setminus \{1\}$ we have

$$\frac{\pi}{p} + \frac{\pi}{q} + \frac{\pi}{r} = \pi. \quad (30)$$

Relation (30) is satisfied for the congruent equilateral triangles $(3, 3, 3)$, the isosceles right triangles $(2, 4, 4)$ and the bisected equilateral triangles $(2, 3, 6)$. Moreover, the only other admissible polygon is the rectangle.

We now study the case of an infinite plane wedge since this is the guiding principle of our investigation. If the angle $\theta = \pi/m$, $m \in \mathbb{N} \setminus \{1\}$ then there is a unique, up to isomorphism, group generated by two involutions $R_{\alpha_1}, R_{\alpha_2}$ such that their product $R_{\alpha_1} \cdot R_{\alpha_2}$ has order m . The group is denoted by Dih_{2m} , called the dihedral group of order $2m$ and has the presentation

$$\text{Dih}_{2m} = \langle R_{\alpha_1}, R_{\alpha_2} \mid R_{\alpha_1}^2 = R_{\alpha_2}^2 = (R_{\alpha_1} \cdot R_{\alpha_2})^m = I \rangle. \quad (31)$$

An alternative way to define Dih_{2m} would be the semidirect product

$$\mathrm{Dih}_{2m} = \mathbb{Z}/m\mathbb{Z} \rtimes \mathbb{Z}/2\mathbb{Z} \quad (32)$$

where if h generates $\mathbb{Z}/2\mathbb{Z}$ then $hgh = g^{-1}$, $\forall g \in \mathbb{Z}/m\mathbb{Z}$. In this set up the presentation reads

$$\text{Dih}_{2m} = \langle g, h \mid h^2 = g^m = (hg)^2 = I \rangle \quad (33)$$

and it can be proved that (33) is equivalent to (31) under the substitutions $R_{\alpha_1} = h$ and $R_{\alpha_2} = hg$. From

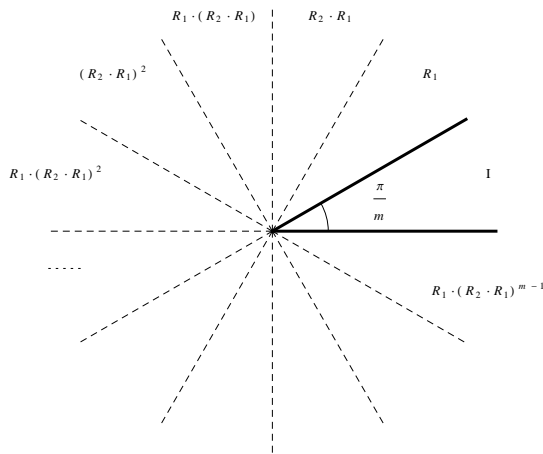


Figure 2: The fundamental region of the infinite wedge with $\theta = \pi/m$ and the virtual domains generated by the elements $R_i \equiv R_{a_i}$ of the group Dih_{2m} .

(32) observe that the dihedral group has the cyclic group $\mathcal{C}_m = \mathbb{Z}/m\mathbb{Z}$ as a subgroup. Also Dih_{2m} is the group of automorphisms of the regular planar m -gon.

Now we adopt the traditional approach to finite reflection groups using root systems. Let us choose the normalised root vectors to be

$$a_1 = (-\sin \theta, \cos \theta)^\top \quad (34)$$

$$a_2 = (0, -1)^\top \quad (35)$$

where “ \top ” stands for the transpose. In general, the reflection of a vector $r \in \mathbb{E}^n$ through a fixed hyperplane $H_a = \{r \in \mathbb{E}^n \mid \langle r, a \rangle = 0\}$ for a given vector $a \neq 0$ is

$$R_a r = r - 2 \frac{\langle a, r \rangle}{\langle a, a \rangle} a \quad (36)$$

where $R_a r = r$, $r \in H_a$ and $R_a r = -r$. The reflection matrices in $n = 2$ are

$$R_{a_1}(\theta) = \begin{pmatrix} \cos(2\theta) & \sin(2\theta) \\ \sin(2\theta) & -\cos(2\theta) \end{pmatrix} \quad \text{and} \quad R_{a_2} = \begin{pmatrix} 1 & 0 \\ 0 & -1 \end{pmatrix}. \quad (37)$$

A simple computation reveals that the element $R_{a_2} \cdot R_{a_1}$, which represents a rotation through twice the angle between the two rays, generates the cyclic group \mathcal{C}_m with elements

$$(R_{a_2} \cdot R_{a_1})^k(\theta) = \begin{pmatrix} \cos(2k\theta) & \sin(2k\theta) \\ -\sin(2k\theta) & \cos(2k\theta) \end{pmatrix}, \quad k = 0, 1, 2, \dots, m-1. \quad (38)$$

Proposition 3.1 *In two dimensions, only the elements of the cyclic group $\mathcal{C}'_m \subset Dih_{2m}$ contribute to the topological constant which appears in the short-time limit of the partition function.*

Proof.

The contribution of elements (38), excluding the identity element (therefore the notation \mathcal{C}'_m), to the trace of the heat kernel is

$$P_t(r, r) = \frac{1}{4\pi t} \sum_{k=1}^{m-1} e^{-\frac{r^2}{t} \sin^2\left(\frac{k\pi}{m}\right)} \quad (39)$$

which when integrated over the infinite angular region in polar coordinates gives

$$\int_0^\infty P_t(r, r) r dr \int_0^{\pi/m} d\theta = \frac{1}{8m} \sum_{k=1}^{m-1} \frac{1}{\sin^2\left(\frac{k\pi}{m}\right)} = \frac{1}{24m} (m^2 - 1). \quad (40)$$

The computation of the finite series in the right-hand side of the first equality of (40) is given in Appendix B. \square

Remarks

1. Relation (40) is time independent whereas if we truncate the wedge using a circle of center the intersection point of the rays and radius R the result becomes time dependent, namely

$$\int_0^R P_t(r, r) r dr \int_0^{\pi/m} d\theta = -\frac{1}{8m} \sum_{k=1}^{m-1} \frac{1}{\sin^2\left(\frac{k\pi}{m}\right)} \left(e^{-\frac{R^2}{t} \sin^2\left(\frac{k\pi}{m}\right)} - 1 \right). \quad (41)$$

Nevertheless the $t \rightarrow 0^+$ limit coincides with (40).

2. If we approximate a circle by an inscribed regular polygon of N vertices then (15) becomes

$$\sum_{i=1}^N \frac{\pi^2 - \phi_i^2}{24\pi\phi_i} = \frac{1}{6} \left(\frac{N-1}{N-2} \right). \quad (42)$$

In (42) as the number of vertices tends to infinity the sum converges to the geometrical constant $1/6$ of (1).

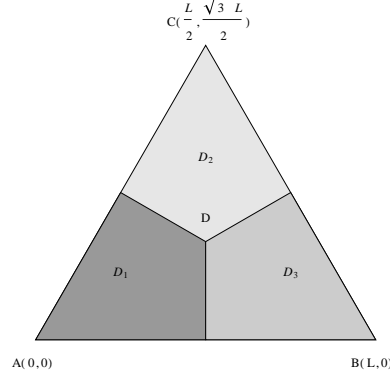


Figure 3: The equilateral triangle is divided with the help of the barycenter D into three subdomains D_i , $i = 1, 2, 3$. The integration is performed over one D_i and the result is multiplied by a factor of three to take into account the overall contribution of the rest D_i 's.

In the sequel we calculate the asymptotic behaviour of the partition function for the equilateral triangle of side length L and show how the reflection elements of Dih_6 group conspire to give the surface area and the length of its perimeter. Each vertex, its two adjacent median points and the centroid form three quadrilateral subdomains (see figure (3)). The Cartesian coordinates of the triangle vertices are

$$A = (0, 0), \quad B = (L, 0), \quad C = \left(\frac{L}{2}, \frac{\sqrt{3}}{2}L \right) \quad (43)$$

and the reflection matrices are given by

$$R_{a_1}\left(\frac{2\pi}{3}\right) = \begin{pmatrix} -\frac{1}{2} & \frac{\sqrt{3}}{2} \\ \frac{\sqrt{3}}{2} & \frac{1}{2} \end{pmatrix} \quad \text{and} \quad R_{a_2} = \begin{pmatrix} 1 & 0 \\ 0 & -1 \end{pmatrix}. \quad (44)$$

The contribution of the identity element I to Z_Ω is

$$\frac{1}{4\pi t} \sum_{i=1}^3 \iint_{D_i} dx dy = \frac{3}{4\pi t} \left(\int_0^{\frac{L}{4}} \int_0^{x\sqrt{3}} dy dx + \int_{\frac{L}{4}}^{\frac{L}{2}} \int_0^{\frac{L-x}{\sqrt{3}}} dy dx \right) = \frac{1}{4\pi t} \sqrt{3} \left(\frac{L}{2} \right)^2 = \frac{1}{4\pi t} |\Omega|, \quad (45)$$

where $|\Omega|$ is the area of the equilateral triangle. The contribution of the reflection elements R_{a_1} , R_{a_2} and $R_{a_1} \cdot R_{a_2} \cdot R_{a_1}$ from the neighbouring to a vertex virtual domains (see figure (4)) is

$$\begin{aligned} \lim_{t \rightarrow 0^+} \left(\sum_{i=1}^3 \iint_{D_i} P_t^{refl.}(x, y) dx dy \right) &= 3 \lim_{t \rightarrow 0^+} \left[\int_0^{\frac{L}{4}} \int_0^{x\sqrt{3}} P_t^{refl.}(x, y) dy dx + \int_{\frac{L}{4}}^{\frac{L}{2}} \int_0^{\frac{L-x}{\sqrt{3}}} P_t^{refl.}(x, y) dy dx \right] \\ &\underset{t \rightarrow 0^+}{\sim} -\frac{|\partial\Omega|}{8\sqrt{\pi t}}, \quad \text{where} \\ P_t^{refl.}(x, y) &= -\frac{1}{4\pi t} \left(e^{-\frac{(\sqrt{3}x-y)^2}{4t}} + e^{-\frac{y^2}{t}} + e^{-\frac{(\sqrt{3}x+y)^2}{4t}} \right) \end{aligned} \quad (46)$$

where the integral identities of Appendix A have been used. The rotations $R_{a_2} \cdot R_{a_1}$ and $(R_{a_2} \cdot R_{a_1})^2$ give

$$\begin{aligned} \lim_{t \rightarrow 0^+} \left(\sum_{i=1}^3 \iint_{D_i} P_t^{rot.}(x, y) dx dy \right) &= 3 \cdot 2 \lim_{t \rightarrow 0^+} \frac{1}{4\pi t} \left[\int_0^{\frac{L}{4}} e^{-\frac{3x^2}{4t}} \left(\int_0^{x\sqrt{3}} e^{-\frac{3y^2}{4t}} dy \right) dx \right. \\ &\quad \left. + \int_{\frac{L}{4}}^{\frac{L}{2}} e^{-\frac{3x^2}{4t}} \left(\int_0^{\frac{L-x}{\sqrt{3}}} e^{-\frac{3y^2}{4t}} dy \right) dx \right] = \frac{1}{3}. \end{aligned} \quad (47)$$

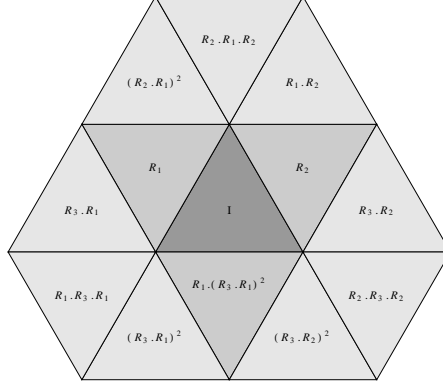


Figure 4: This figure depicts the virtual domains generated by the elements of the Dih_6 group for an equilateral triangle neglecting the next to neighbours regions.

Remarks

1. Due to the defining relations (31) one can prove the following identities

$$R_{a_1} \cdot R_{a_2} \cdot R_{a_1} = R_{a_2} \cdot R_{a_1} \cdot R_{a_2}, \quad (R_{a_2} \cdot R_{a_1})^2 = R_{a_1} \cdot R_{a_2}. \quad (48)$$

Such relations support the simplification of the computations and depend on the anticlockwise (or clockwise) orientation of the reflections.

2. Applying (40) the topological terms for the triangles $(2, 4, 4)$, $(2, 3, 6)$ and for the rectangle are $3/8$, $5/12$ and $1/4$ respectively. Comparing the values of the topological term we establish the decreasing sequence

$$c_{\text{rectangle}} < c_{(3,3,3)} < c_{(2,4,4)} < c_{(2,3,6)}. \quad (49)$$

Inequalities (49) indicate that the topological term is minimised by squares (or rectangles) while the equilateral triangles saturate the lowest bound among all acceptable triangles as one can prove by using the method of Lagrange undetermined multipliers.

3.3 The $n = 3$ case

In three dimensions the bounded regions compatible with the image method are: triangular prisms with $(\theta_{12}, \theta_{23}, \theta_{31}) = (\frac{\pi}{3}, \frac{\pi}{2}, \frac{\pi}{2})$, right triangular prisms (both with five faces) and rectangular parallelepipeds (six faces). Again we study the infinite trihedral angle by applying the image method to determine the time independent term in Z_Ω . Let θ_{ij} denote the angle between the i - and j -plane (see figure (5)). The reflection matrices associated with the roots α_i , $i = 1, 2, 3$ orthogonal to the i -planes are found to be

$$R_{a_1}(\theta_{12}, \theta_{31}) = \begin{pmatrix} 1 - 2 \sin^2 \theta_{12} \sin^2 \theta_{31} & \sin(2\theta_{12}) \sin^2 \theta_{31} & \sin \theta_{12} \sin(2\theta_{31}) \\ \sin(2\theta_{12}) \sin^2 \theta_{31} & 1 - 2 \cos^2 \theta_{12} \sin^2 \theta_{31} & -\cos \theta_{12} \sin(2\theta_{31}) \\ \sin \theta_{12} \sin(2\theta_{31}) & -\cos \theta_{12} \sin(2\theta_{31}) & -\cos(2\theta_{31}) \end{pmatrix} \quad (50)$$

$$R_{a_2}(\theta_{23}) = \begin{pmatrix} 1 & 0 & 0 \\ 0 & \cos(2\theta_{23}) & \sin(2\theta_{23}) \\ 0 & \sin(2\theta_{23}) & -\cos(2\theta_{23}) \end{pmatrix} \quad (51)$$

$$R_{a_3} = \begin{pmatrix} 1 & 0 & 0 \\ 0 & 1 & 0 \\ 0 & 0 & -1 \end{pmatrix} \quad \text{where} \quad (\theta_{12}, \theta_{23}, \theta_{31}) = \left(\frac{\pi}{p}, \frac{\pi}{q}, \frac{\pi}{r}\right), \quad p, q, r \in \mathbb{N} \setminus \{1\}. \quad (52)$$

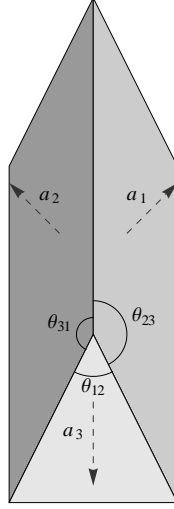


Figure 5: The angles θ_{ij} and the roots a_i orthogonal to the i -plane.

The interior of the trihedral domain does not contain any virtual mirror generated by multiple reflections in the three bounding hyperplanes only if (p, q, r) (or permutation of them) satisfy

$$\frac{\pi}{p} + \frac{\pi}{q} + \frac{\pi}{r} > \pi \quad \text{and} \quad r, q, p \in \mathbb{N} \setminus \{1\}. \quad (53)$$

The solutions of (53) are

$$(2, 2, r), \quad (2, 3, 3), \quad (2, 3, 4), \quad \text{and} \quad (2, 3, 5). \quad (54)$$

The defining relations of the corresponding group become

$$(R_{a_1})^2 = (R_{a_2})^2 = (R_{a_3})^2 = (R_{a_1} \cdot R_{a_2})^p = (R_{a_2} \cdot R_{a_3})^q = (R_{a_3} \cdot R_{a_1})^r = I. \quad (55)$$

Proposition 3.2 *If the infinite trihedral angle is $(\theta_{12}, \theta_{23}, \theta_{31}) = (\frac{\pi}{r}, \frac{\pi}{2}, \frac{\pi}{2})$, $r \in \mathbb{N} \setminus \{1, 2\}$ then only the elements of $\mathcal{C}'_r \times \{R_{a_3}\} \subset Dih_{2m} \times \mathbb{Z}/2\mathbb{Z}$ contribute to the constant term of Z_Ω . In this case the contribution reads*

$$I_{const.}(r) = -\frac{1}{32r} \sum_{k=1}^{r-1} \frac{1}{\sin^2(\frac{k\pi}{r})} = -\frac{1}{96r}(r^2 - 1). \quad (56)$$

Proof.

Setting $\theta_{12} = \frac{\pi}{r}$ and $\theta_{23} = \theta_{31} = \frac{\pi}{2}$ into relations (50), (51) we obtain

$$R_{a_1} = \begin{pmatrix} \cos(\frac{2\pi}{r}) & \sin(\frac{2\pi}{r}) & 0 \\ \sin(\frac{2\pi}{r}) & -\cos(\frac{2\pi}{r}) & 0 \\ 0 & 0 & 1 \end{pmatrix}, \quad R_{a_2} = \begin{pmatrix} 1 & 0 & 0 \\ 0 & -1 & 0 \\ 0 & 0 & 1 \end{pmatrix}. \quad (57)$$

The elements of $\mathcal{C}'_r \times \{R_{a_3}\}$ have the matrix representation

$$(R_{a_1} \cdot R_{a_2})^k \cdot R_{a_3} = \begin{pmatrix} \cos(\frac{k\pi}{r}) & -\sin(\frac{k\pi}{r}) & 0 \\ \sin(\frac{k\pi}{r}) & \cos(\frac{k\pi}{r}) & 0 \\ 0 & 0 & -1 \end{pmatrix}, \quad k = 1, \dots, r-1 \quad (58)$$

and are related to reflections. Applying the proposition of Appendix A we end up with the trace heat kernel formula

$$P_t(x, y, z) \sim - \left(\frac{1}{4\pi t} \sum_{k=1}^{r-1} e^{-\frac{1}{t} \sin^2(\frac{k\pi}{r})(x^2+y^2)} \right) \left(\frac{1}{\sqrt{4\pi t}} e^{-\frac{z^2}{t}} \right). \quad (59)$$

The observed factorization is due to the direct product nature of the group $\mathcal{C}'_r \times \{R_{a_3}\}$. Integration over the infinite trihedral angle produces (56). \square

The rest of the group elements give the following transition densities:

Reflections		Rotations	
Group Element	$(4\pi t)^{\frac{3}{2}} P_t(x, y, z)$	Group Element	$(4\pi t)^{\frac{3}{2}} P_t(x, y, z)$
R_{a_1}	$-e^{-\frac{1}{t}(\sin(\frac{\pi}{r})x - \cos(\frac{\pi}{r})y)^2}$	$(R_{a_1} \cdot R_{a_2})^k, k = 1, \dots, r-1$	$e^{-\frac{1}{t} \sin^2(\frac{k\pi}{r})(x^2+y^2)}$
R_{a_2}	$-e^{-\frac{y^2}{t}}$	$R_{a_3} \cdot R_{\alpha_1}$	$e^{-\frac{1}{t}[(\sin(\frac{\pi}{r})x - \cos(\frac{\pi}{r})y)^2 + z^2]}$
R_{a_3}	$-e^{-\frac{z^2}{t}}$	$R_{a_3} \cdot R_{\alpha_2}$	$e^{-\frac{(y^2+z^2)}{t}}$

(60)

According to Coxeter's classification scheme there are polyhedra which fall into the class of three-dimensional tessellations but the method of images puts severe constraints on the admissible ones through the requirement $\theta_{ij} = \pi/p_{ij}$, $p_{ij} \in \mathbb{N} \setminus \{1\}$, $\forall i, j$. An example is the three tetrahedra (0123), (0023) and (0033) (see figure (6)). In particular for the (0123) tetrahedron we have the angle $10_{\text{left}}3_{\text{up}} \simeq 54.73^\circ$.

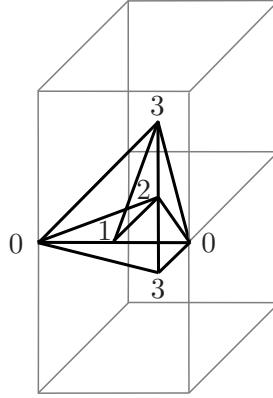


Figure 6: The symbol $(ijkl)$ denotes the tetrahedron with edges (ij) , (jk) , (kl) . The coordinates of the points $\{0, 1, 2, 3\}$ are: $0_{\text{left}} = (0, 0, 0)$, $0_{\text{right}} = (L, 0, 0)$, $3_{\text{up}} = (\frac{L}{2}, \frac{L}{2}, \frac{L}{2})$, $3_{\text{down}} = (\frac{L}{2}, \frac{L}{2}, -\frac{L}{2})$, $1 = (\frac{L}{2}, 0, 0)$, $2 = (\frac{L}{2}, \frac{L}{2}, 0)$. The length of each side is given by $\overline{(ij)} = \frac{(00)}{2} \sqrt{j-i}$, $j > i$.

The first candidate in our investigation is the prism $(\theta_{12}, \theta_{23}, \theta_{31}) = (\frac{\pi}{3}, \frac{\pi}{2}, \frac{\pi}{2})$ which in the light of proposition (3.2) gives the topological term $-1/6$. The asymptotic behaviour of the partition function is found to be

$$Z_{\Omega, (2,2,3)}(t) \stackrel{t \rightarrow 0^+}{\sim} \frac{\sqrt{3}a^2c}{4(4\pi t)^{\frac{3}{2}}} - \frac{a(a\sqrt{3}/2 + 3c)}{16\pi t} + \frac{3(2a + c)}{32\sqrt{\pi t}} - \frac{1}{6} \quad (61)$$

where a is the side length of the equilateral triangle and c the height of the prism.

The next candidates are the right triangular prisms with $(\theta_{12} = \theta_{23} = \theta_{31} = \frac{\pi}{2})$ at two vertices. We distinguish the following two possibilities

$$Z_{\Omega, (2,4,4)}(t) \stackrel{t \rightarrow 0^+}{\sim} \frac{a^2c}{2(4\pi t)^{\frac{3}{2}}} - \frac{a(a + c(2 + \sqrt{2}))}{16\pi t} + \frac{2a(2 + \sqrt{2}) + 3c}{32\sqrt{\pi t}} - \frac{3}{16} \quad (62)$$

$$Z_{\Omega, (2,3,6)}(t) \stackrel{t \rightarrow 0^+}{\sim} \frac{a^2c\sqrt{3}}{2(4\pi t)^{\frac{3}{2}}} - \frac{a(a\sqrt{3} + c(3 + \sqrt{3}))}{16\pi t} + \frac{2a(3 + \sqrt{3}) + 3c}{32\sqrt{\pi t}} - \frac{5}{24} \quad (63)$$

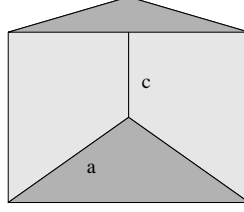


Figure 7: The right triangular prism.

where a in (63) is the length of the side opposite to the $\pi/6$ angle and c as in the previous case.

Finally, we study the rectangular parrallelepiped with edge lengths (a, b, c) . Dividing it into eight sub-rectangular parrallelepipeds we arbitrarily choose one of them and perform our computation. Their contributions are listed in the following table:

Reflections		Rotations	
Group Element	Contribution	Group Element	Contribution
R_{α_1}	$-\frac{bc}{64\pi t} \operatorname{erf}\left(\frac{a}{2\sqrt{t}}\right)$	$R_{\alpha_1} \cdot R_{\alpha_2}$	$\frac{c}{64\sqrt{\pi t}} \operatorname{erf}\left(\frac{a}{2\sqrt{t}}\right) \operatorname{erf}\left(\frac{b}{2\sqrt{t}}\right)$
R_{α_2}	$-\frac{ac}{64\pi t} \operatorname{erf}\left(\frac{b}{2\sqrt{t}}\right)$	$R_{\alpha_3} \cdot R_{\alpha_1}$	$\frac{b}{64\sqrt{\pi t}} \operatorname{erf}\left(\frac{a}{2\sqrt{t}}\right) \operatorname{erf}\left(\frac{c}{2\sqrt{t}}\right)$
R_{α_3}	$-\frac{ab}{64\pi t} \operatorname{erf}\left(\frac{c}{2\sqrt{t}}\right)$	$R_{\alpha_3} \cdot R_{\alpha_2}$	$\frac{a}{64\sqrt{\pi t}} \operatorname{erf}\left(\frac{b}{2\sqrt{t}}\right) \operatorname{erf}\left(\frac{c}{2\sqrt{t}}\right)$

(64)

The identity element again gives the volume of the domain, the reflection elements R_{a_i} , $i = 1, 2, 3$ provide the area of the bounding surfaces, the rotations contribute to the lengths of the edges and the reflection $R_{a_1} \cdot R_{a_2} \cdot R_{a_3}$ supports the topological term. In the short-time limit the error functions converge to unity and if we sum up the contributions from all the vertices we recover the correct result

$$Z_{\Omega}(t) \stackrel{t \rightarrow 0^+}{\sim} \frac{abc}{(4\pi t)^{\frac{3}{2}}} - \frac{2(ab + bc + ac)}{16\pi t} + \frac{4(a + b + c)}{32\sqrt{\pi t}} - \frac{1}{8}. \quad (65)$$

Again depending on the shape of the polytope we observe the following decreasing sequence of values for the topological term

$$c_{\text{rec. par.}} < c_{(2,2,3)} < c_{(2,4,4)} < c_{(2,3,6)}. \quad (66)$$

4 Conclusions

In this paper we studied systematically the short-time asymptotics of the free partition function corresponding to the Dirichlet Laplacian on tessellations which possess mirror symmetry through the hyperplanes bounding the domain. The method of images was effectively applied up to three-dimensions. The analysis was simplified significantly since the number of polytopes fulfilling the reflection constraint was limited. We established that the geometrical quantities $|\Omega|, |\partial\Omega|$ and the topological term are associated with specific elements of the orthogonal group. This method can be generalised to higher dimensions and may help to solve the same problem with Dirichlet fractional Laplacians without requiring the knowledge of its spectra.

Appendix A

Proof of (15)

For a polygon $P = \nu_1\nu_2 \cdots \nu_m$ in \mathbb{E}^2 the curvature of P at each interior vertex ν_i is the real number

$$k_{\nu_i} = \angle(\overrightarrow{\nu_{i-1}\nu_i}, \overrightarrow{\nu_i\nu_{i+1}}) = \theta_i \quad (\text{A.1})$$

which represents the angle between the vectors $\overrightarrow{\nu_{i-1}\nu_i}$ and $\overrightarrow{\nu_i\nu_{i+1}}$. The global (or total curvature) of a polygon is defined to be the sum of angles of its consecutive edges [14]

$$\mathcal{K}(P) = \sum_{i=1}^{m-2} \angle \overrightarrow{\nu_i\nu_{i+1}}, \overrightarrow{\nu_{i+1}\nu_{i+2}}. \quad (\text{A.2})$$

Using the well-known result [4] that $\mathcal{K}(P) = 2\pi$ for a polygonal planar, convex and closed curve in \mathbb{E}^2 , it is trivial to prove (15). \square

Proposition 4.1 *The Euclidean norm of the vector $r - Gr$ with $G \in \mathbb{O}(m)$ is given by*

$$\|r - Gr\|^2 = \begin{cases} 2r^\top(I - G)r, & \text{for } G \text{ being a symmetric matrix} \\ 2r^\top(I - \text{diag}(G))r, & \text{for } G \text{ having an antisymmetric component} \end{cases} \quad (\text{A.3})$$

and “ $^\top$ ” denotes transpose.

Proof.

Bearing in mind that G is orthogonal ($G^\top = G^{-1}$), it is easily proved that

$$\|r - Gr\|^2 = 2r^2 - r^\top(G + G^\top)r. \quad (\text{A.4})$$

If G is symmetric then $G^\top = G$ and $G + G^\top = 2G$. If G can be written as a sum $G = \text{diag}(G) + A$ with $A^\top = -A$ then $G + G^\top = 2\text{diag}(G)$. \square

In the computations we have made extensive use of the following integral representation of the error function and integrals involving the error function, exponentials and powers [15]

$$\text{erf}(az) = \frac{2}{\sqrt{\pi}} \int_0^{az} e^{-u^2} du = \frac{2az}{\sqrt{\pi}} \int_0^1 e^{-a^2 z^2 u^2} du, \quad z = \text{Re } z + i\text{Im } z = x + iy \quad (\text{A.5})$$

$$\int_0^\infty \text{erf}(ax) e^{-b^2 x^2} dx = \frac{\sqrt{\pi}}{2b} - \frac{1}{b\sqrt{\pi}} \tan^{-1}\left(\frac{b}{a}\right) \quad (\text{A.6})$$

$$\int_0^\infty x \text{erf}(ax) e^{-b^2 x^2} dx = \frac{a}{2b^2} \frac{1}{\sqrt{a^2 + b^2}}, \quad \text{Re}(b^2) > \text{Re}(a^2), \text{Re}(b^2) > 0. \quad (\text{A.7})$$

Appendix B

Proof of $\sum_{k=1}^{m-1} \frac{1}{\sin^2(\frac{k\pi}{m})} = \frac{1}{3}(m^2 - 1)$

The finite sum is written equivalently as

$$\sum_{k=1}^{m-1} \frac{1}{\sin^2(\frac{k\pi}{m})} = m - 1 + \sum_{k=1}^{m-1} \cot^2\left(\frac{k\pi}{m}\right) \quad (\text{B.1})$$

therefore it is enough to prove that the second sum equals $(m-1)(m-2)/3$. Using simple trigonometric identities we obtain

$$\sum_{k=1}^{m-1} \cot^2\left(\frac{k\pi}{m}\right) = - \sum_{k=1}^{m-1} \left(\frac{1 + \omega^k}{1 - \omega^k}\right)^2, \quad \omega = e^{\frac{2i\pi}{m}}. \quad (\text{B.2})$$

Define the function

$$((x)) := \begin{cases} x - [x] - \frac{1}{2}, & x \notin \mathbb{Z} \\ 0, & \text{otherwise} \end{cases} \quad (\text{B.3})$$

In our case $[k/m] = 0$ since $m \geq 2$ and $k = 1, 2, \dots, m-1$. The function $((l/m))$ has period m therefore it can be expanded in finite Fourier series as

$$\left(\left(\frac{l}{m}\right)\right) = \sum_{k=0}^{m-1} \hat{f}(k) \omega^{kl}, \quad \text{where} \quad \hat{f}(k) = \frac{1}{m} \sum_{l=0}^{m-1} \left(\frac{l}{m} - \frac{1}{2}\right) \omega^{-kl}. \quad (\text{B.4})$$

The Fourier coefficients turn out to be

$$\hat{f}(k) = \begin{cases} 0, & k = 0 \\ \frac{1}{2m} \left(\frac{1+\omega^k}{1-\omega^k}\right), & \text{for } k, m \text{ coprime, positive integers} \end{cases} \quad (\text{B.5})$$

using the summation formulas [5]

$$\sum_{l=1}^{m-1} l = \frac{1}{2}m(m-1), \quad \sum_{l=1}^{m-1} lx^l = \frac{1-x^m}{(1-x)^2} - \frac{mx^m}{1-x}, \quad \sum_{l=0}^{m-1} \omega^{-kl} = 0. \quad (\text{B.6})$$

Applying the convolution theorem for finite Fourier series

$$(f * g)(l) = \sum_{n=0}^{m-1} f(l-n)g(n) = m \sum_{n=0}^{m-1} \hat{f}(n)\hat{g}(n)\omega^{ln} \quad (\text{B.7})$$

for $l = 0$ and $f = g$ we get

$$(f * f)(0) = - \sum_{n=0}^{m-1} f^2(n) = m \sum_{n=0}^{m-1} \hat{f}^2(n) \quad (\text{B.8})$$

where the minus sign is justified by the fact that the cotangent function is odd. Thus (B.1) becomes

$$\sum_{k=1}^{m-1} \cot^2\left(\frac{k\pi}{m}\right) = 4m \sum_{n=1}^{m-1} \left(\frac{n}{m} - \frac{1}{2}\right)^2 = \frac{1}{3}(m-1)(m-2) \quad (\text{B.9})$$

using the formula $\sum_{l=1}^{m-1} l^2 = m(m+1)(2m+1)/6$. □

References

- [1] H.S.M. Coxeter, *Regular Polytopes*, Methuen and Co. LTD., London, 1948.
- [2] H.S.M. Coxeter and W.O.J. Moser, *Generators and Relations for Discrete Groups*, Springer-Verlag, 1984.
- [3] E.B. Davies, *Heat Kernels and Spectral Theory*, Cambridge University Press, 1989.
- [4] W. Fenchel, *Über Krümmung und Windung geschlossener Raumkurven*, Math. Ann. 101, 238-252 (1929).
- [5] I.S. Gradshteyn and I.M. Ryzhik, *Table of Integrals, Series, and Products*, Academic Press, 1994, 5th edition.
- [6] A. Hatzinikitas, *The Partition Function of the Dirichlet Operator $\mathcal{D}_{2s} = \sum_{i=1}^d (-\partial_i^2)^s$ on a d -Dimensional Rectangle Cavity*, arXiv: 1403.0204.
- [7] C. Itzykson, *Simple Integrable Systems, and Lie Algebras*, Int. J. Mod. Phys. A, 1, (1986) 65-115.
- [8] C. Itzykson and J.M. Luck, *Arithmetical Degeneracies in Simple Quantum Systems*, J. Math. A: Math. Gen., 19, (1986) 211-239.

- [9] M. Kac, *Can one hear the shape of a drum?*, Amer. Math. Monthly 73 (1966) 1-23.
- [10] R. Kane, *Reflection Groups and Invariant Theory*, Springer-Verlag, New York, 2001.
- [11] J.B. Keller, *The scope of the image method*, Com. Pure Appl. Math., vol. VI (1953) 505-512.
- [12] B.J. McCartin, *Eigenstructure of the Equilateral Triangle, Part I: The Dirichlet Problem*, SIAM Review, 45 (2003) 267-287.
- [13] H.P. McKean, I.M. Singer, *Curvature and the eigenvalues of the Laplacian*, J. Differential Geometry 1 (1967) 43-69.
- [14] J.M. Morvan, *Generalised Curvatures*, Springer-Verlag, 2008.
- [15] E.W. Ng and M. Geller, *A Table of Integrals of the Error Functions*, Journal of Research of the National Bureau of Standards - B. Mathematical Sciences, Vol. 73B, No. 1, January - March, 1969.
- [16] A. Pleijel, *A study of certain Green's functions with applications in the theory of vibrating membranes*, Ark. Mat. 2 (1954), 553-569.